INTERNATIONAL JOURNAL OF RENEWABLE ENERGY RESEARCH
M. Mansori and Z. Malika, Vol. 9, No. 3, September, (2019)

Grid Connected Photovoltaic Energy Conversion System Modeling and Control Using SMC-BSC Approach

Mansori Mohamed‡, Zazi Malika

Research Center STIS, ERERA, Department of Electrical Engineering, Higher Normal School of Technical Education, Mohammed V University, Rabat, BP 6207, Morocco
(Mohamed.mansori@um5s.net.ma , M.zazi@um5s.net.ma)

‡ Corresponding Author; Mansori Mohamed, Higher Normal School of Technical Education, Mohammed V University, Rabat, BP 6207, Morocco
Tel: +2126 3825 5753, Mohamed.mansori@um5s.net.ma

Received: 10.07.2019 Accepted: 17.08.2019

Abstract- The photovoltaic generators are characterized by a nonlinear electrical characteristics that admit one only maximum power point (MPP). Therefore, the maximum power point tracking (MPPT) is very essential to improve the photovoltaic systems efficiency. This paper presents a robust method to control and optimization of a grid-connected photovoltaic (PV) energy conversion system .The control design is based on a nonlinear sliding mode control (SMC)-Backstepping control (BSC) approach. The principal aim of this work is to develop the sliding mode technique for having a grid-connected PV system with a goods performances. The SMC is ameliorated by associate it with the Backstepping technique, it is applied to track the maximum power from the PV panels, and also, to ensure an independent control of the active (P) and reactive (Q) powers. In this control strategy the stability is verified by the Lyapunov approach. The simulations results has been realized in Simulink/Matlab and they have shown that the proposed system present a good robustness with the SMC-BSC method.

Keywords- Photovoltaic system; MPPT technique; Optimization; Sliding mode control; Backstepping control; SMC-BSC method.

1. Introduction

The photovoltaic technology can be considered a good solution to the growing demand of electricity, because of , it is natural, free, abundant, does not pollute the atmosphere, it avoid nuclear risks, and, it is independent of fossil fuels that are poorly distributed and exhaustible. The demand of energy produced from photovoltaic systems is significantly increase, the research shows that the photovoltaic systems contribution of electric energy production was about 14000 MW in 2010, and should be 70 000 MW in 2020 [1].

The photovoltaic modules are defined by their current/voltage and power/voltage characteristics, that are non-linear and depend on the climatic conditions and the load, and they admit one optimum operating point. For this reason, it is necessary to track the maximum power to maximize the PV system efficiency and optimize the energy transfer in the production chain. Electrically, the photovoltaic systems optimization is performed by a commands called MPPT methods.

In the literature, many MPPT techniques have been developed with a DC/DC boost converter for tracking the photovoltaic system (PV) maximum power [2, 3]. These methods consist of to search the voltage at the maximum power point, and this, whatever the weather conditions and load.

In [4], the voltage open circuit method (VOC) is used to find the PV generator voltage at the maximum power point (MPP), this strategy is based on a linear approximation of the open-circuit voltage and the voltage at the MPP. The same thing between the current at the MPP and the short-circuit current, as demonstrated in [5]. These methods are simple and economical but they are not able to adapt to climate change.

The perturbation and observation method (P&O) is presented in [6], this algorithm is based on the MPP search by raising and lowering incrementally the PV module voltage. It is mostly used due to its simplicity, but it presents an undesirable oscillations around the maximum power. The conductance incremental method is used in [7] to PV system optimize, this control is based on the search of the MPP through the search a null derivative of the PV system power.

The disadvantage of this command resides in its complexity and instability.

To interconnect a photovoltaic system with a three-phase grid-tied, it is necessary to ensure the maximum energy transfer with a very good quality. To accomplish these objective: the photovoltaic generator voltage must track the maximum power point, the DC-Bus voltage shall be regulated in a fixe desired value ,and the delivered currents to grid must have a sinusoidal shape and in phase with the alternating voltages. There are many grid-side converter control strategies have been developed to control independently active and reactive power transferred from the DC circuit to the grid. PI, PID controllers are generally used to control the grid-tied inverters [8]. However, PI and PID controller cannot eliminate the sinusoidal signals error in the steady state. Sliding mode control (SMC) is an effective controller based on a variable structure control strategy developed to remove these negative effects in nonlinear systems. It has a robust control, simple application and fast response features under the exchange of all system parameters.

Generally in SMC control approach, the control law is composed of two parts: the equivalent component and the discontinuous component. The first one represents the dynamic of the system during the sliding mode and the other represents the system dynamic during the convergence mode. However, in the convergence regime, the undesirable chattering can be caused by the discontinuous component, this control signal component is based on a complicated choice of a gain to ensure the system convergence towards its desired state. Therefore, to resolve this ripples problem, a Backstepping control (BSC) using with sliding mode control has been proposed, consequently, the control law second component that caused the oscillations problem in sliding mode will be changed by the Backstepping control low. The RL filter is usually used to eliminate currents harmonics caused by pulse width modulation (PWM) of the grid-side converter.

The objective of this work is to contribute to the optimization and control of a grid-connected photovoltaic energy conversion system. This contribution concerns two mains points:

- The study of a non-linear approach based on SMC-BSC method to extract the maximum power from a PV generator and to control of the injected active (P) and reactive (Q) powers in the grid.
- Have a non-isolated DC/ DC converter and DC/AC inverter with good efficiencies and high voltage gains.

This work is organized as follows: in the section 2, a general system description is briefly presented. The section 3 is dedicated to modeling of the proposed system. The section 4 is reserved for the SMC-BSC control application to grid-connected photovoltaic energy conversion system control. The simulation results are presented in section 5. Finally, some conclusions of this work are summarized in section 6.

2. Proposed system description

The proposed system consists the elements: the photovoltaic generator (PV panels), the DC-DC boost converter, the grid-tied three phase inverter, the RL filter to eliminate the currents harmonics ,and ,the controller system designed by SMC-BSC approach to track the maximum power from the PV panels and to control the PV energy injected to grid. The synoptic diagram of this is depicted in Figure 1.

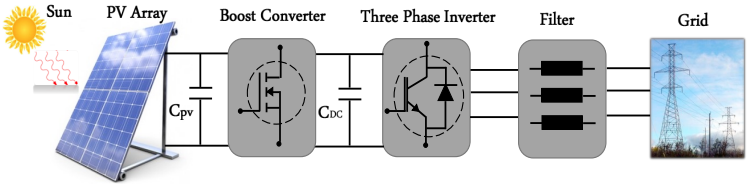

Fig. 1. Proposed system structure.

3. Proposed system modeling

3.1. Photovoltaic panel model

An ideal solar cell is electrically modelled by a current source in parallel with a diode. However, no solar cell is ideal. Therefore, two resistances are added to the model: one mounted in series and the other in parallel as it is shown in the following figure:

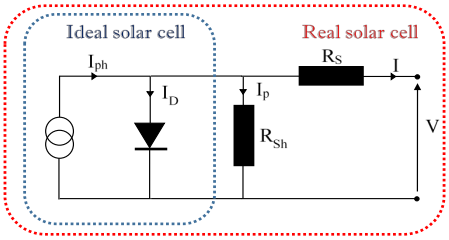

Fig. 2. Solar cell electrical model.

In the model above, the diode (D) characterizing the PN junction, the current source characterizing the photo-current I_{ph}, the series resistance R_s representing the losses by effect Joule, and the shunt resistance R_{sh} characterizing the leakage currents that flowing in the grids. Therefore, the current-voltage characteristic of the PV cell is given hereafter:

$$I = I_{ph} - I_D - I_p = I_{Ph} - I_0\left[\exp\left(\frac{V + R_S.I}{V_t}\right) - 1\right] - \frac{V + R_S.I}{R_{sh}} \quad (1)$$

Practically, this equation can be simplified by considering that the resistance R_{sh} has a high value, thus the current I_p can be neglected. The equation. 1 becomes:

$$I = I_{Ph} - I_0\left[\exp\left(\frac{V + R_S.I}{V_t}\right) - 1\right] \quad (2)$$

Therefore, the PV panel mathematical model, that contains N_p columns of N_s cells connected in series, is represented by the following equation:

$$I = N_p I_{Ph} - N_p I_0 \left[\exp\left(\frac{V + R_S.I}{N_s.V_t} \right) - 1 \right] \quad (3)$$

Where:

- The thermodynamic potential V_t :

$$V_t = \frac{KTA}{q} \quad (4)$$

- The photo-current I_{ph} :

$$I_{Ph} = [I_{scr} + K_i(T - 298)\ ] * \frac{G}{1000} \quad (5)$$

- The current of reverse saturation of the diode:

$$I_{rs} = \left(\frac{I_{scr}}{\exp\left(\frac{qV_{oc}}{N_s kAT} \right) - 1} \right) \quad (6)$$

- The saturation current of the diode:

$$I_0 = I_{rs} \left[\frac{T}{298} \right]^3 \exp\left[\left(q * \frac{Eg_0}{kA} \right) \left(\frac{1}{298} - \frac{1}{T} \right) \right] \quad (7)$$

3.2. Boost converter model :

The boost converter is primarily consisted by a switch K (MOSFET or IGBT) and a diode D, its conductions are complementary, when K is closed D is opened and vice-versa. The switch K is commanded by a pulse width modulation signal (PWM). To modeling the boost converter, the Kirchhoff's laws is applied to its electrical circuit represented thereafter:

Fig. 3. Boost converter circuit.

Depending on the condition of K, The electrical circuit is characterized by two functioning sequences:

First sequence is characterized by u = 1, K is closed and D is opened. The converter equations are given as:

$$\begin{cases} \frac{di_L}{dt} = \frac{V_{pv}}{L} \\ \frac{dV_{DC}}{dt} = -\frac{I_{Inv}}{C_{DC}} \end{cases} \quad (8)$$

Second sequence is characterized by u = 0, K is opened and D is closed. The converter equations system is presented as:

$$\begin{cases} \frac{di_L}{dt} = \frac{V_{pv}}{L} - \frac{V_{DC}}{L} \\ \frac{dV_{DC}}{dt} = -\frac{I_{Inv}}{C_{DC}} + \frac{i_L}{C_{DC}} \end{cases} \quad (9)$$

From equation (8) and (9), the boost converter mathematical model is:

$$\begin{cases} \frac{di_L}{dt} = \frac{V_{pv} - V_{DC}}{L} + \frac{V_{DC}}{L}.u \\ \frac{dV_{DC}}{dt} = -\frac{I_{Inv}}{C_{DC}} + \frac{i_L}{C_{DC}} - \frac{i_L}{C_{DC}}.u \end{cases} \quad (10)$$

We take $x = [x_1, x_2]^T = [I_L, V_{DC}]^T$, the expression (10) can be rewrite as follows:

$$\begin{cases} \frac{dx_1}{dt} = \frac{V_{pv} - x_2}{L} + \frac{x_2}{L}.u \\ \frac{dx_2}{dt} = -\frac{I_{Inv}}{C_{DC}} + \frac{x_1}{C_{DC}} - \frac{x_1}{C_{DC}}.u \end{cases} \quad (11)$$

Then

$$\dot{x} = \frac{dx}{dt} = f_B(x,t) + g_B(x,t)u + h_B \quad (12)$$

Where:

$$f_B(x,t) = \begin{bmatrix} 0 & \frac{-x_2}{L} \\ \frac{x_1}{C_{DC}} & 0 \end{bmatrix}, g_B(x,t) = \begin{bmatrix} \frac{x_2}{L} \\ \frac{-x_1}{C_{DC}} \end{bmatrix}, h_B = \begin{bmatrix} \frac{V_{PV}}{L} \\ \frac{-I_{inv}}{C_{DC}} \end{bmatrix}$$

3.3. Grid-tied inverter model :

The grid-tied three phase inverter and equivalent circuit are shown in Fig. 4. The inverter consists of a DC voltage source (V_{DC}), six power switches (S1-- S6), line filter (R_g-L_g).

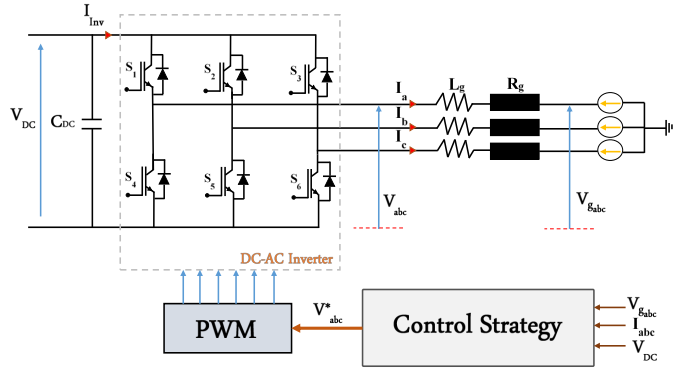

Fig. 4. Grid connected system structure.

According to Fig. 4 , the relationship between, the grid voltages, the inverter voltages and line currents in the stationary reference is given as follows [9, 10]:

$$\begin{cases} V_a = L_g \dfrac{dI_a}{dt} + R_g I_a + V_{ga} \\ V_b = L_g \dfrac{dI_b}{dt} + R_g I_b + V_{gb} \\ V_c = L_g \dfrac{dI_c}{dt} + R_g I_c + V_{gc} \end{cases} \quad (13)$$

In the park referential, equation system (13) becomes:

$$\begin{cases} V_d = L_g \dfrac{dI_d}{dt} + R_g I_d + V_{gd} - L_g w I_q \\ V_q = L_g \dfrac{dI_q}{dt} + R_g I_q + V_{gq} + L_g w I_d \end{cases} \quad (14)$$

The active and reactive power injected by the photovoltaic generator in the grid can be defined for a balanced three-phase system as follows:

$$\begin{cases} P = \dfrac{3}{2}\left(V_{gd}.I_d + V_{gq}.I_q\right) \\ Q = \dfrac{3}{2}\left(V_{gq}.I_d - V_{gd}.I_q\right) \end{cases} \quad (15)$$

Considering the line currents as a state vectors and the inverter voltages as a command vectors, the equation system (14) can be expressed in the state representation form as follows:

$$L_g \dot{x} = f_g(x,t) + g_g(x,t)u + h_g \quad (16)$$

With:

$$u = \left[V_d, V_q\right]^T = \left[u_1, u_2\right]^T \quad \text{and} \quad x = \left[I_d, I_q\right]^T = \left[x_1, x_2\right]^T$$

Therefore, the grid-tied inverter model is deducted as follows:

$$\begin{cases} L_g \dfrac{dx_1}{dt} = u_1 - V_{gd} - R_g x_1 + L_g w x_2 \\ L_g \dfrac{dx_2}{dt} = u_2 - V_{gq} - R_g x_2 - L_g w x_1 \end{cases} \quad (17)$$

Then, the expression (16) can be rewrite as follows:

$$L_g \begin{bmatrix} \dot{x}_1 \\ \dot{x}_2 \end{bmatrix} = f_g(x,t) + g_g(x,t)u + h_g \quad (18)$$

Where:

$$f_g(x,t) = \begin{bmatrix} -R_g & L_g w \\ -L_g w & -R_g \end{bmatrix} \cdot \begin{bmatrix} x_1 \\ x_2 \end{bmatrix},$$

$$g_g(x,t) = \begin{bmatrix} 1 \\ 1 \end{bmatrix} \text{ and } h_g = \begin{bmatrix} -V_{gd} \\ -V_{gq} \end{bmatrix}$$

3.4. Sliding mode control strategy:

The sliding mode controller synthesis can be decomposed of multiple steps :

- The sliding surface choice :

The sliding surface $S(x)$ represents the desired dynamic of the studied system. The general equation used to determine the sliding surface that ensures the convergence of the controlled variable to its reference value is given by [11]:

$$S(x) = \left(\frac{\partial}{\partial t} + \lambda_x\right)^{r-1} e(x) \quad (19)$$

Where:

e (x) : is the difference between the controlled variable and its reference $e(x) = x_{ref} - x$.

λ_x *:* is a positive constant.

r : relative degree.

- The sliding mode existence:

The existence condition of sliding regime S(x) = 0 is deduced by applying the Lyapunov's stability criterion:

$$\lim_{S \to 0} S.\dot{S} \prec 0 \quad (20)$$

- The control law determination :

The sliding mode control (u) is consists of two terms: a discontinuous control term depending on the sliding surface sign (u_n) and an equivalent control term (u_{eq}) characterizing the system dynamic in the sliding regime:

$$u = u_{eq} + u_n \tag{21}$$

Considering the system described by the following equation:

$$\dot{x} = f(x,t) + g(x,t).u \tag{22}$$

The sliding surface derivative is given by:

$$\dot{S} = \nabla S.\dot{x} + \frac{\partial S}{\partial t} = \nabla S.f(x,t) + \nabla S.g(x,t)u + \frac{\partial S}{\partial t} \tag{23}$$

Where: ∇S is the gradient of S.

The equivalent command that maintains the state trajectory on the sliding surface, is obtained by the resolution of equation $\dot{S} = 0$, and it is expressed as follows:

$$u_{eq} = -\left[\nabla S.g(x,t)\right]^{-1}.\left[\nabla S.f(x,t) + \frac{\partial S}{\partial t}\right] \tag{24}$$

u_n is determined by Lyapunov equation to guarantee the stability of the controlled system, and its expression is given as [11]:

$$u_n = K.sign(S) \tag{25}$$

The gain K is chosen positive to satisfy the convergence condition. $\dot{S}.S \prec 0$

3.5. Sliding mode control SMC- Backstepping control BSC approach:

The sliding mode control has the advantage of be efficacy to bring the studied system at the desired state no matter his initial state and despite the perturbations. But it has a major problem of oscillations during the transitory regime (the convergence mode), this oscillations is caused by the gain choice of the command attractive component.

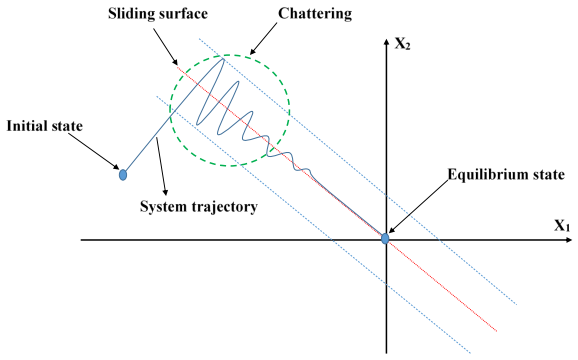

Fig. 5. Chattering phenomenon.

The choice of this gain is very influential, because, if it is very small the response time will be very long and, if it is chosen very large, a strong oscillations will be produced in the controller. These oscillations can provoke the damage of the control organ and excite the neglected dynamics (Chattering phenomenon), as showing in Fig. 5.

To improve the sliding mode control, many solutions has been proposed, in [12, 13, and 14] the second order sliding mode controller based on super-twisting algorithm has been used, this method is based on to change the attractive component expression by another expression similar to that of a PI corrector. In [15], a sliding mode control (SMC) - direct power controller (DPC) is presented, this technique is based on the association of the sliding mode control with the direct power control technique.

In this work to eliminate the oscillations caused by the attractive component of the sliding mode control, an association of this method with the Backstepping command (BSC) has been proposed, this technique consists of replacing the attractive component of the sliding mode command by that found using the backstepping technique. So, the control law using sliding mode control (SMC)-Backstepping control (BSC) approach, is expressed as follows:

$$u_{SBC} = u_{S-eq} + u_{BSC} \tag{26}$$

With:

u_{SBC} : The global command of system.

u_{S-eq} : The equivalent component of the control law obtained by sliding mode control.

u_{BSC} : The control law obtained by Backstepping control.

4. Application of Sliding mode (SMC)-Backstepping (BSC) approach to control and optimization of three phase grid-connected photovoltaic (PV) system

The aim of this part is to design a control laws for:

- Extract the maximum power from the photovoltaic generator.
- Regulate the DC-link voltage in the inverter input.
- Inject the sinusoidal currents in phase with the voltages by obtaining a unity power factor.

4.1. SMC-BSC control application to track the photovoltaic generator maximum power :

a. Calculation of the sliding mode control equivalent component :

The maximum power point MPP of the PV system is characterized by:

$$\frac{dP_{pv}}{dV_{pv}} = 0 \tag{27}$$

The first step to design the control law is the choice of the sliding surface, which can be selected using the following equation:

$$S(x) = \frac{dP_{pv}}{dV_{pv}} = I_{pv} + \frac{dI_{pv}}{dV_{pv}}.V_{pv} \quad (28)$$

The figure bellow represents the Power/Voltage characteristic of photovoltaic generator

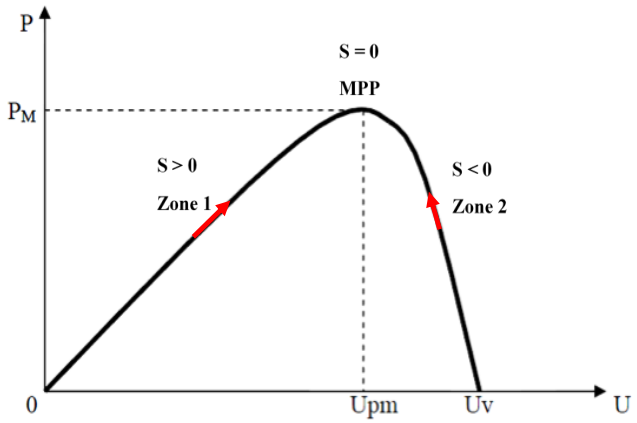

Fig.6. Typical Power-Voltage characteristic.

This characteristic can be divided of two zones separated by the point MPP (S(x) = 0). Zone 1 is characterized by a positive slope (S(x) > 0), and zone 2 that characterized by a negative slope (S(x) < 0). If, for example, the operating point (OP) is in left of the MPP, The command must move it to the sliding surface by incrementing the voltage V_{pv} .If on the contrary, the OP is in right of the MPP, the command must move the OP towards the sliding surface by decrementing the tension V_{pv} . Therefore, the adopted control to track the maximum power point is given as follows:

$$u = \begin{cases} 0 & If \quad S \succ 0 \\ 1 & If \quad S \prec 0 \end{cases} \quad (29)$$

From equation (24), the equivalent control term u_n applied to the boost converter is given as:

$$u_{S-eq} = 1 - \frac{V_{pv}}{V_{DC}} \quad (30)$$

b. Calculate of the Backstepping control law to track the maximum power point of the PV photovoltaic generator

The first step in the control law synthesis using the backstepping approach is to define the dynamic error expression, so, from the power-voltage characteristic of the PV generator, the desired state to track the maximum power is defined by:

$$e_p = \frac{\partial P_{pv}}{\partial V_{pv}} = I_{pv} + \frac{\partial I_{pv}}{\partial V_{pv}}.V_{pv} \quad (31)$$

In the second step, to ensure the stability of system in the steady state, the lyapunov function is defined by:

$$V = \frac{e_p^{\,2}}{2} \quad (32)$$

$$\dot{V} = -k_v.e_p^{\,2} = e_p.\dot{e}_p \qquad (k_v \succ 0) \quad (33)$$

Therefore, the error expression become:

$$e_p = -\frac{2}{k_v}\frac{\partial I_{pv}}{\partial t} - \frac{1}{k_v}\frac{\partial}{\partial t}\left(\frac{\partial I_{pv}}{\partial V_{pv}}\right).V_{pv} \quad (34)$$

From the equations (11) and (34), the control law based on backstepping approach applied to the boost converter for the maximum power extraction is:

$$u_{BSC} = 1 - \frac{V_{pv}}{V_{DC}} - \frac{L}{2V_{DC}}\left[\frac{\partial}{\partial t}\left(\frac{\partial I_{pv}}{\partial V_{pv}}\right).V_{pv} + k_v.e_p\right] \quad (35)$$

c. SMC-BSC control law to Track the Photovoltaic generator maximum power:

From the equations (26), (30) and (35) the global expression of SMC-BSC control law to track the maximum power point from the PV generator is giving as:

$$u_{SBC} = 2 - 2.\frac{V_{pv}}{V_{DC}} - \frac{L}{2V_{DC}}\left[\frac{\partial}{\partial t}\left(\frac{\partial I_{pv}}{\partial V_{pv}}\right).V_{pv} + k_v.e_p\right] \quad (36)$$

d. Verification of the sliding mode existence:

In the sliding mode control, the Lyapunov function is defined as shown in the following equation [9]:

$$V(x) = \frac{1}{2}S(x)^2 \quad (37)$$

The surface S(x) is attractive when the Lyapunov derivative is negative (attractiveness condition):

$$\dot{V}(x) = \dot{S}(x).S(x) \le 0 \ , \ \forall S(x) \ne 0 \quad (38)$$

To demonstrate the sliding mode existence as presented in equation (38), the both zones illustrated in figure 5 are considered and the derivative of S(x) is calculated from the equation (28):

$$\dot{S}(x) = -\left(2 + \frac{V_{pv}}{N_s.V_t}\right)\frac{N_p.I_{sc}}{N_s.V_t}\exp\left(\frac{V_{pv} - N_s.V_{oc}}{N_s.V_t}\right)\frac{dV_{pv}}{dt} \quad (39)$$

- Zone 1 : $S(x) > 0$

If the OP is on the zone 1, the voltage must be increased to reach the MPP. That means that $\frac{dV_{pv}}{dt} > 0$. So $\dot{S}(x) < 0$, and $S(x).\dot{S}(x) < 0$.

- Zone 2 : $S(x) < 0$

If the OP is on the zone 2, the voltage must be decreased to reach the MPP. That means that $\frac{dV_{pv}}{dt} < 0$. So $\dot{S}(x) > 0$, and $S(x).\dot{S}(x) < 0$.

We conclude that the sliding mode exists, and the system is asymptotically stable whatever the operating point localization. The applied control law forces the system trajectory to converge toward the sliding surface in a finished time, and to remain it on the sliding surface until the equilibrium point.

4.2. SMC-BSC control application to Active-Reactive powers control of three-phase grid-connected PV solar system:

a. DC Link voltage regulation :

The sliding surface that allows to have a desired value of DC link voltage can be expressed by:

$$S(x) = e_S(x) + k_{is}\int_0^t e_S(x).dt \tag{40}$$

With: $$e_S(x) = V^*{}_{DC} - V_{DC}$$

The equivalent component of sliding mode approach is obtained by applied the invariance law in the sliding regime:

$$\dot{S}(x) = (\dot{V}_{DC})^* - \frac{I_C}{C_{DC}} + k_{is}.e_S(x) = 0 \tag{41}$$

The control vector chosen to regulate the DC link voltage is the I_C current that defined by the following expression:

$$I_C = \dot{V}_{DC}.C_{DC} \tag{42}$$

Therefore, from the equation (41) the equivalent component of I_C current can be expressed by:

$$I_{S-Ceq} = C_{DC}.((\dot{V}_{DC})^* + k_{is}e_S(x)) \tag{43}$$

To expresses the backstepping component, the dynamic error of regulation is chosen by:

$$e_B(x) = (V_{DC}{}^* - V_{DC}) + k_{ib}\int_0^t (V_{DC}{}^* - V_{DC}).dt \tag{44}$$

The backstepping control law is obtained from the lyapunov condition of stability expressed in equations (32) and (33):

$$-k_V e_B(x) = \dot{V}_{DC}{}^* - \frac{I_C}{C_{DC}} + k_{ib}(V_{DC}{}^* - V_{DC}) \tag{45}$$

Consequently, the backstepping component of I_C current will be expressed by:

$$I_{BSC} = C_{DC}.(\dot{V}_{DC}{}^* + k_{ib}(V_{DC}{}^* - V_{DC}) + k_V e_B(x)) \tag{46}$$

Therefore, from the equation (46) and (43), the control law based on SMC-BSC approach is expressed by:

$$I_{SBC} = C_{DC}.\left[2.\dot{V}_{DC}{}^* + (k_{ib} + k_{is}).(V_{DC}{}^* - V_{DC}) + k_V e_B(x))\right] \tag{47}$$

The flowing figure represents the bloc schema of this control strategy:

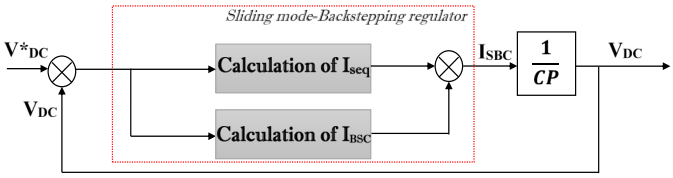

Fig.7. DC link voltage regulation schema bloc.

b. Active (P) – Reactive (Q) powers control:

From the equations (15), the active (P) – reactive (Q) powers control is very complexes by the four grandeurs: I_d ,I_q ,V_d , and V_q .Therefore, to decouple and simplify the active and reactive powers control, applying the voltage orientation technique to the d-axis, then we can write:

$$\begin{cases} V_{gd} = V_g \\ V_{gq} = 0 \end{cases} \tag{48}$$

Using the simplifications above, the equation (15) become:

$$\begin{cases} P = \frac{3}{2}\left(V_g.I_d\right) \\ Q = -\frac{3}{2}\left(V_g.I_q\right) \end{cases} \tag{49}$$

According to the equation (49), the active power can be controlled by the current I_d, and the reactive power can be controlled by the current I_q, then, the sliding surfaces chosen to control the active and reactive power is given as:

$$\begin{cases} S(I_d) = I^*_d - I_d \\ S(I_q) = I^*_q - I_q \end{cases} \quad (50)$$

To calculate the equivalent component, we applying the invariance condition in the sliding regime:

$$\begin{cases} \dot{S}(I_d) = \dot{I}^*_d - \frac{1}{L_g}(V_d - V_{gd} - R_g.I_d + L_g.w.I_q) = 0 \\ \dot{S}(I_q) = \dot{I}^*_q - \frac{1}{L_g}(V_q - V_{gq} - R_g.I_q - L_g.w.I_d) = 0 \end{cases} \quad (51)$$

Therefore, the inverter voltages is expressed as follows:

$$\begin{cases} V_{dS-eq} = \dot{I}^*_d.L_g + V_{gd} + R_g.I_d - L_g.w.I_q \\ V_{qS-eq} = \dot{I}^*_q.L_g + V_{gq} + R_g.I_q + L_g.w.I_d \end{cases} \quad (52)$$

To calculate the backstepping component of active and reactive power control, the dynamic errors is chosen as:

$$\begin{cases} e_d = I^*_d - I_d \\ e_q = I^*_q - I_q \end{cases} \quad (53)$$

From the equation (32), the lyapunov functions is given by:

$$\begin{cases} V_d = \frac{e_d^2}{2} \\ V_q = \frac{e_q^2}{2} \end{cases} \quad (54)$$

The lyapunov condition of stability is expressed as flowing:

$$\begin{cases} -k_d.e_d^2 = e_d.\dot{e}_d \\ -k_q.e_q^2 = e_q.\dot{e}_q \end{cases} \quad (k_d \succ 0 \text{ and } k_q \succ 0) \quad (55)$$

Then, the inverter voltages is expressed as follows:

$$\begin{cases} V_{dBS} = \dot{I}^*_d.L_g + V_{gd} + R_g.I_d - L_g.w.I_q + L_g.k_d.e_d \\ V_{qBS} = \dot{I}^*_q.L_g + V_{gq} + R_g.I_q + L_g.w.I_d + L_g.k_q.e_q \end{cases} \quad (56)$$

Therefore, the control law based on SMC-BSC approach is expressed by:

$$\begin{cases} V_{dSBC} = 2.\left[\dot{I}^*_d.L_g + V_{gd} + R_g.I_d - L_g.w.I_q\right] + L_g.k_d.e_d \\ V_{qSBC} = 2.\left[\dot{I}^*_q.L_g + V_{gq} + R_g.I_q + L_g.w.I_d\right] + L_g.k_q.e_q \end{cases} \quad (57)$$

The block diagram of active and reactive power control strategy is showing in the Fig. 8.

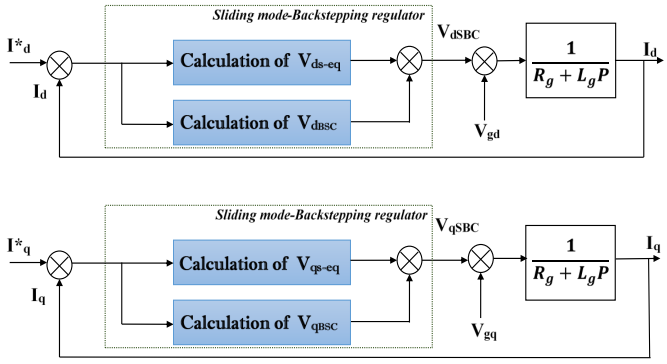

Fig.8. Active and Reactive power regulation schemas bloc.

Therefore, the overall block diagram of the PV system with the proposed control strategy is shown in Figure below:

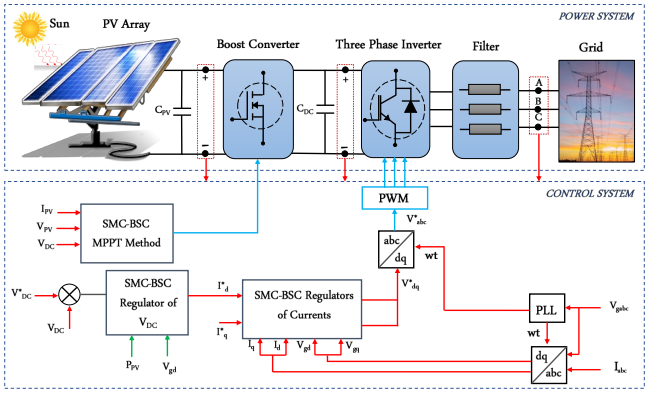

Fig.9. Synoptique diagram of the PV system with proposed control strategy.

5. Simulation results:

To analyze the performance of the SMC-BSC strategy applied to control and optimize a three phase grid-connected photovoltaic (PV) system, a variable profiles of irradiation and temperature are considered in this simulation. The PV system parameters are presented in the table 1.

Table 1. PV system Parameters.

PV Model : SPR-305E-WHT-D	
Maximum power	P_{mpp} = 305 W
Voltage of maximal power	V_{mpp} = 54.7 V
Current of maximal power	I_{mpp} = 5.58 A
Open-circuit Voltage	V_{oc} =64.2 V
Short-circuit current	I_{sc} = 5.96 A
Cell numbers	96(1×96)
Temperature coefficient of the maximum power	- 0.470%
Band-gap energy of silicon	E_{go} = 1.1 EV
Temperature coefficient of the short-circuit current	K_i = 0.061745%A/°C
Reference temperature	T_r = 25°C
Boltzmann Constant	K = $1.3805*10^{-23}$ J/K
Electron charge	q = $1.6 * 10^{-19}$ C
Diode ideality factor	A = 0.94504
Shunt resistance	R_{sh} =969.5934 ohms
Series resistance	R_s=0.37152 ohms
PV Array	
Parallel strings	N_p = 66
Series-connected modules per string	N_s = 5
Maximum power	P_{max} = 100 Kw
DC-DC boost converter	
C_{pv}=100e-6 F L= 5e-3 H C_{DC}=6000e-06 F	
Filter	
L_g = 0.28e-3 H R_g = 0.125 ohms	
Grid	
Phase-to-phase voltage	U_g=400v
Frequency	F=50 Hz

MPPT Controller parameters
K_v = 1000
Active – Reactive powers controller parameters
K_v = 9, K_{is} = 30, K_{ib} = 30 K_d = 9e5 F_p = 9753Hz

5.1. DC side simulations results:

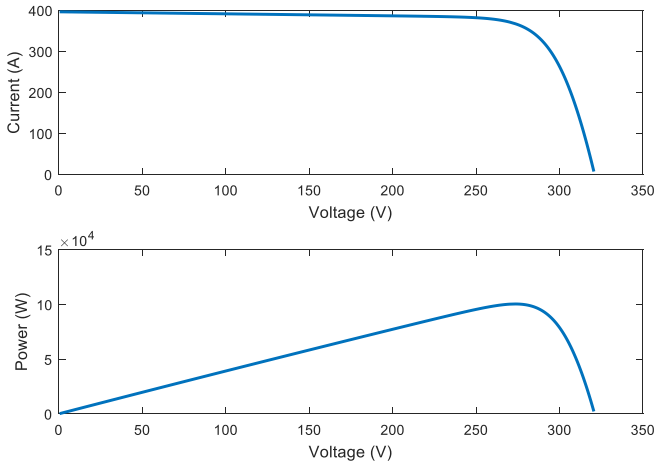

Fig.10. PV Array Characteristics.

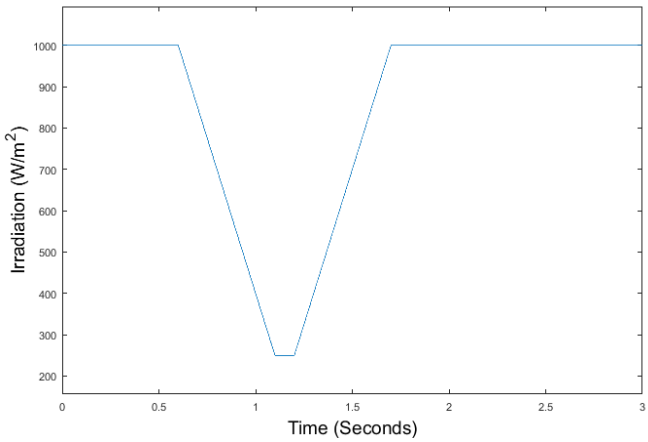

Fig.11. Irradiation profile.

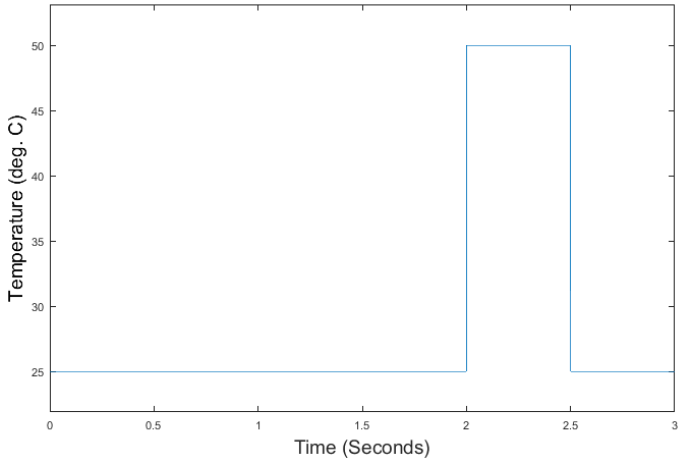

Fig.12. Temperature profile.

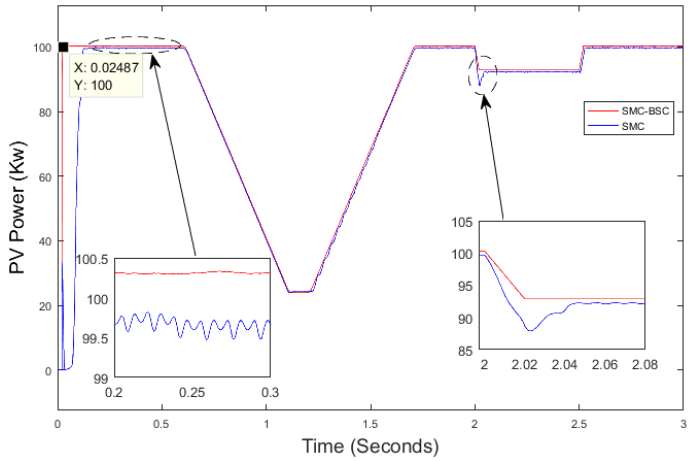

Fig.13. Photovoltaic power output.

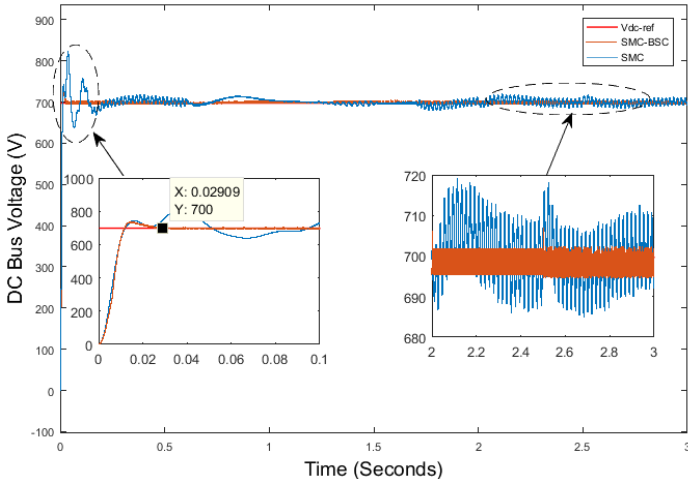

Fig.14. DC Bus voltage.

5.2. AC side simulations results:

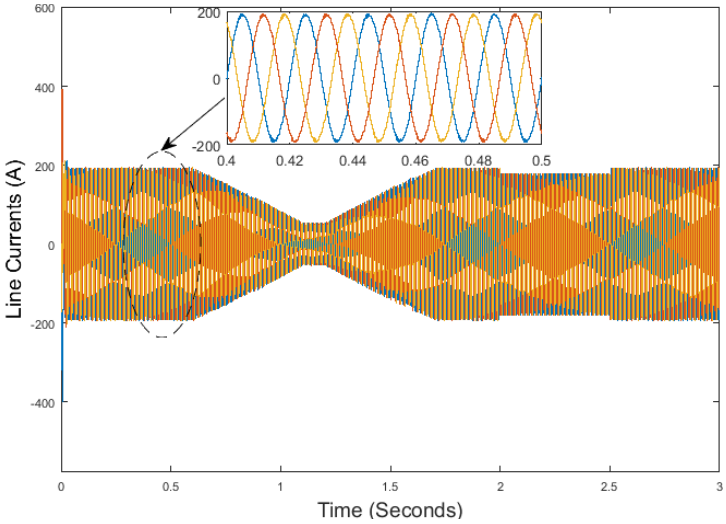

Fig.15.injected line currents using SMC-BSC.

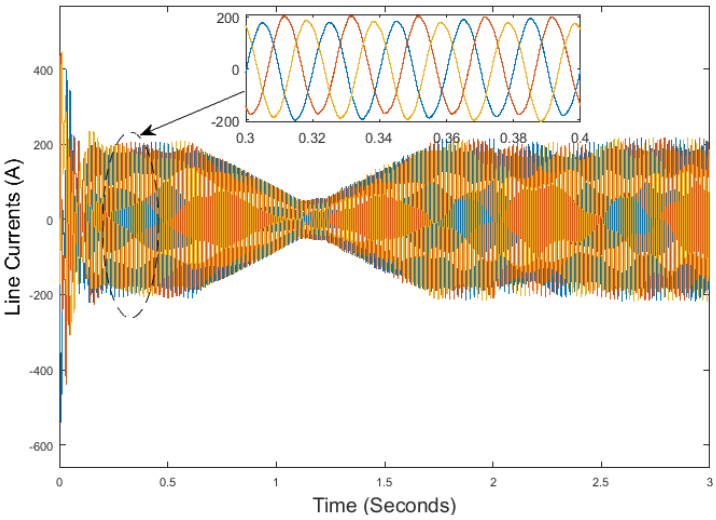

Fig.16.injected line currents using SMC.

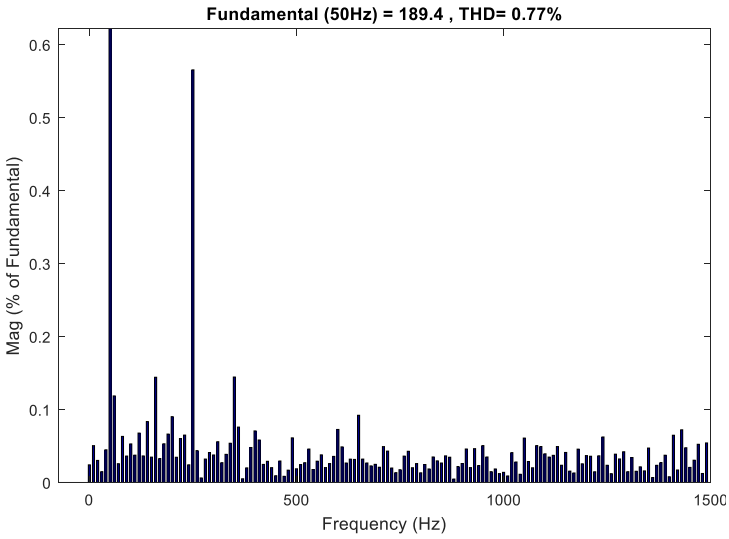

Fig.17. Line current FFT analysis using SMC-BSC.

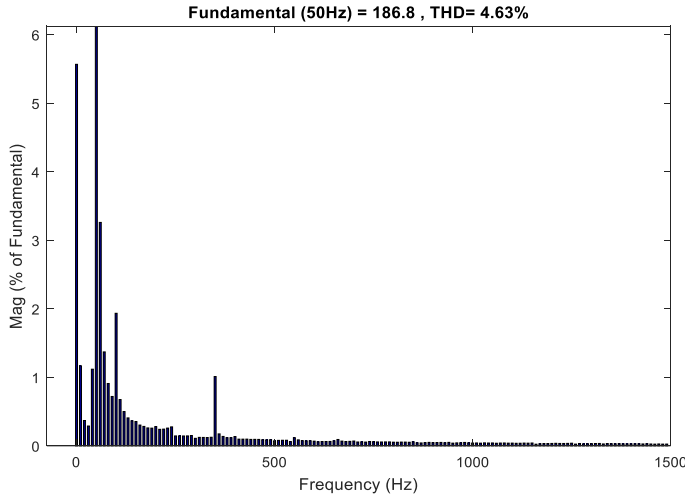

Fig.18. Line current FFT analysis using SMC.

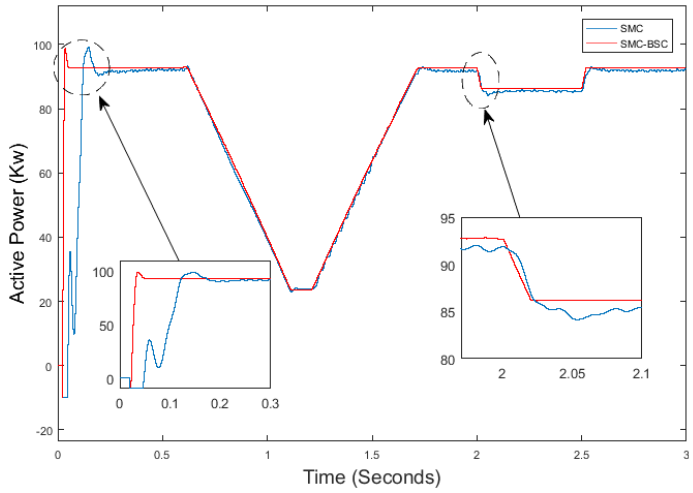

Fig.19. Active power.

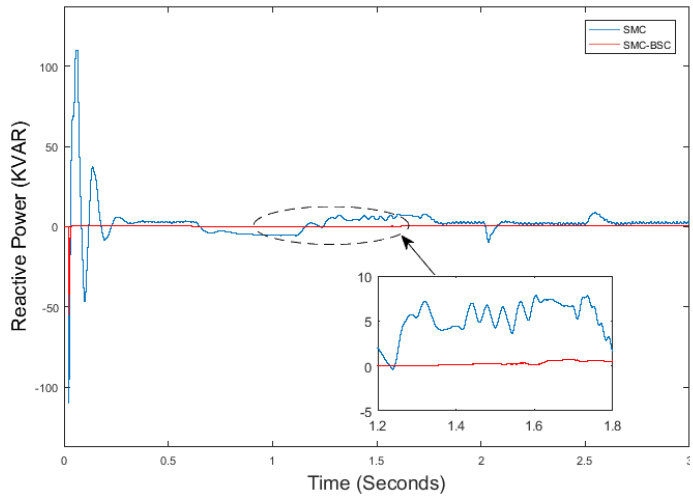

Fig.20. Reactive power.

5.3. Discussions:

For the DC side simulations results, the Fig.10 shows the PV array characteristics in the STC conditions (Irr=1000 W/m2 and T=25 deg.C). Based on the Fig. 13, it is clear that the PV power output track the maximum power that depends on the irradiation and temperature profiles showed in Fig.11 and Fig.12. The Fig.14 illustrates the DC bus voltage with a good dynamic response, which are continuous and approximately constant.

From the AC side simulations results, the Fig.15, shows the injected line currents with good quality, it presents a negligible total harmonic distortion (THD = 0.77%) as shown in Fig17. Active and reactive powers of system are given by Fig.19 and Fig.20. We can see that P and Q follow their references with high dynamic response that proving that the SMC-BSC control capable to ensure independent control of P and Q with a good compensation of the reactive power. Thus, the proposed system based on SMC-BSC approach present a high-performances of P-Q decoupling and reactive power compensation with a very low THD (0.77%).

5.4. The SMC-BSC approach robustness :

The objective of this work is to visualize the performance and the robustness of the SMC-BSC approach compared to SMC method. Therefore, a comparative study between SMC-BSC and SMC techniques has been done in this paper. To do this, all rsimulation results of the comparative study obtained are summarized in the following tables:

Table 2. DC side comparison results.

Command technique	SMC	SMC-BSC
Response time	124 ms	24 ms
Output power oscillation amplitude	0.31 Kw	0.025 Kw
Losses energy when there is a change of irradiation	0.12 KJ	0 J

Table 3. AC side comparison results.

Command technique	SMC	SMC-BSC
Active power oscillation amplitude	1.2 Kw	0.15 Kw
Reactive power oscillation amplitude	1.4 Kvar	0.21 Kvar
THD	4.63 %	0 .77 %

From these results, it can be concluded easily that the SMC-BSC has enormous advantages compared to SMC method, it provides to achieve the steady state in a very short time of the milliseconds order, with a reduced oscillation and an acceptable THD value.

6. Conclusion:

In this study SMC-BSC algorithm is proposed to control and optimization of a grid-connected PV energy conversion

system. The aim of this control strategy is to develop the classically SMC technique by replacing its normal component causing the chattering phenomena with the control law obtained using the backstepping approach. In the proposed system the SMC-BSC technique has used to design the MPPT algorithm applied to the boost converter for extract the maximum power from the PV generator, and based on the theoretical and simulations results, it is clear that the SMC-BSC technique has an advantage to track the maximum power point with good response time and with reduced oscillations. Also, this technique is used to control the active and reactive powers injected in the grid, to do this, the voltage orientation technique is exploited to simplify the control of injected powers, and consequently, the output DC voltage is regulated to calculate the reference of direct current component to control the active power, and the quadratic current component is oriented to zero for having the null reactive power and an unity factor power. Stability in this control strategy is always vitrified by the Lyapunov function according to the control law. The simulations results indicate that the proposed strategy enables to ensure an excellent control of the DC Bus voltage, and a maximization of the produced powers from PV arrays with a good performance. The main contribution of this work has been appeared with the designing of the SMC-BSC approach. The proposed controller has good response time and very stable in steady-state conditions. SMC-BSC technique is recognized with their simplicity of topology and their high performances. This theory was applied to satisfy all recommendations of grid-connected generation power systems control behaviours. The results prove that the system enable to ensure a high-quality of P-Q control with good decoupling, satisfactory of the reactive power compensation moreover, an excellent power factor.

Acknowledgements

This work has been supported by Scientific and Technical Research National Centre (CNRST), Rabat, Morocco.

References

[1] M. Seyedmahmoudian, B. Horan, T. K. Soon, R. Rahmani, A. M. Than Oo, S. Mekhilef, and A. Stojcevski, “State of the art artificial intelligence-based MPPT techniques for mitigating partial shading effects on PV systems - A review,” Renew. Sustain. Energy Rev., vol. 64, pp. 435–455, 2016.

[2] S. Ould-Amrouche, D. Rekioua, A. Hamidat, Modelling photovoltaic water pumping systems and evaluation of their CO2 emissions mitigation potential, Applied Energy 87 (2010) 3451–3459.

[3] Hurng-Liahng Jou, Wen-Jung Chiang, Jinn-Chang Wu, A novel maximum power point tracking method for the photovoltaic system, conference international PEDS, pp: 619-623, 2007.

[4] M.A.S. Masoum, H. Dehbonei, Design, construction and testing of a voltage-based maximum power point tracker (VMPPT) for small satellite power supply. In: 13th Annual AIAA/USU Conference, SmallSatellite1999.

[5] T. Noguchi, S. Togashi, R. Nakamoto, Short-current pulse-based adaptive maximum power point tracking for a photovoltaic power generation system. Proceedings of the 2000 IEEE International Symposium on ISIE 2000; 1: 157 – 162.

[6] L. J.L. Santos, F. Antunes, A. Chehab and C. Cruz, A Maximum Power Point Tracker for PV Systems Using a High Performance Boost Converter. Solar Energy2006; 80(7): 772 – 778.

[7] Krauter, Stefan C. W., Solar Electric Power Generation - Photovoltaic Energy Systems, Springer Edition; 2006

[8] Kesler M, Kisacikoglu MC, Tolbert LM. Vehicle-to-grid reactive power operation using plug-in electric vehicle bidirectional offboard charger. Ind Electron IEEE Trans 2014; 61(12):6778e84.

[9] J.J.SLOTINE, « Sliding controller design for non linear systems », IJC, vol. 2, 1984, pp 421- 434.

[10] H. Komurcugil, “Adaptive terminal sliding-mode control strategy for DC–DC buck converters”, ISA Transactions vol.51, 2012, pp.673-681.

[11] H. Guldemir, “Sliding mode control of DC–DC boost converter”, Journal of Appleid Sciences 5 (3), 2005, pp.588-592.

[12] Tsang, K. M., and J. Wang. “Design of second order sliding mode controller for synchronous generators based on singular perturbation method”, Power System Technology, 2002. Proceedings. Power Con 2002. International Conference on, 1, pp. 333-338, (2002).

[13] Levant, Arie. “Sliding order and sliding accuracy in sliding mode control”, International journal of control, 58(6), pp. 1247-1263, (1993).

[14] Laghrouche, S. “Robust second order sliding mode control for a permanent magnet synchronous motor”, American Control Conference, 2003.Proceedings of the 2003. 5, pp.4071-4076, (2003).

[15] Ozbay H, SMC-DPC based active and reactive power control of grid-tied three phase inverter for PV systems, International Journal of Hydrogen Energy (2017).